Journal of Organometallic Chemistry 880 (2019) 317–321

Contents lists available at ScienceDirect

Journal of Organometallic Chemistry

journal homepage: www.elsevier.com/locate/jorganchem

Facile synthesis and optoelectronic exploration of silylthiophene substituted benzodithiophene polymer for organic field effect transistors

Chinna Bathula [a, *], Henry Opoku [a], Abhijit Kadam [b], Nabeen K. Shrestha [a], Taegweon Lee [a, c], Yong-Young Noh [a, **]

[a] Department of Energy and Materials Engineering, Dongguk University, Seoul 04620, Republic of Korea
[b] Department of Chemical and Biochemical Engineering, Gachon University, Seongnam City, Seoul, 461-701, Republic of Korea
[c] Nanowearble Co. Ltd, 30 Pildong-ro, 1-gil, Jung-gu, Seoul, 04620, Republic of Korea

ARTICLE INFO

Article history:
Received 10 August 2018
Received in revised form
1 November 2018
Accepted 9 November 2018
Available online 10 November 2018

Keywords:
Benzodithiophene
Diketopyrrolopyrrole
Stille reaction
Copolymer
OFET

ABSTRACT

This work reports the synthesis, characterization and organic field effect transistors (OFET) application of a novel conjugated polymer (**PBDTDPP**) based on silylthiophene substituted benzo[1,2-b:4,5-b′]dithiophene (BDT) donor and diketopyrrolopyrrole (DPP) acceptor obtained *via* Stille polymerization reaction. The polymer exhibits a broad absorption in the UV–visible spectrum ranging from 300 nm to 900 nm with the band edge of the polymer at 1.31 eV. Thermogravimetric analysis of the polymer demonstrates the stability up to 303 °C, and the cyclic voltammetry shows the HOMO and LUMO levels at −5.42 and −4.11 eV, respectively. Employing the polymer as an active layer in a bottom gate-top contact based OFET, hole mobility of as high as 9.34×10^{-2} $cm^2 V^{-1} s^{-1}$ with the On/Off ratio of ~10^4 was obtained. This work successfully demonstrates that the DPP and the silylthiophene substituted BDT are promising units to build D-A based copolymer for organic electronics.

1. Introduction

Organic materials offer the attractions of solution processing and compatibility with plastic substrates, enabling the development of flexible electronics. Organic thin-film transistors (OTFTs) are essential building blocks for large-area, flexible, and low-cost organic electronics, which offers promising applications in technology areas, such as light-weight and flexible displays; radio-frequency identification (RFID) circuitry [1]; and physical, chemical, and biological sensors [2]. The ultimate success of OTFTs requires developing organic semiconductors that allow i) efficient charge transport, which is characterized by high field-effect mobility; ii) solution-based processing for low-cost fabrication; and iii) good operational stability of devices under ambient air, moisture, and light exposure. A major challenge in printed electronics technology is reproducibly building homogeneous large-area organic semiconductor thin films with high charge carrier mobilities. Despite its high expectation, performances of the organic devices had been lower than those of conventional inorganic-based electronic devices. However, continuous research efforts have contributed to the great advances in the performance of, in particular, OFETs and OPVs during the last several years [3].

Conjugated polymer backbones containing alternating electron rich donor and electron-poor acceptor units have emerged as a common approach in the design of low band gap materials [4]. By careful consideration of the repeating donor and acceptor units, control over the highest occupied molecular orbital (HOMO) and lowest unoccupied molecular orbital (LUMO) energy levels of these polymers are possible [5]. This facilitates the design of a variety of chromophores with high charge transport in OFETs and optimal light absorption properties, thereby enhancing the efficiency of polymer solar cells [6–9]. This is mainly due to polymers exhibiting closer intermolecular π - π stacking in view of the attractive forces between the donor and acceptor units.

Although the large number of high performing materials have been explored for OFETs, diketopyrrolopyrrole remains as one of the most versatile and widely used structural motifs [10]. Other

* Corresponding author.
** Corresponding author.
E-mail addresses: cdbathula@gmail.com (C. Bathula), yynoh@dongguk.edu (Y.-Y. Noh).

https://doi.org/10.1016/j.jorganchem.2018.11.013
0022-328X/

class of materials such as thieno [3,2-b]thiophene [11], benzo[1,2-b:4,5-b′]dithiophene(BDT) [12–15], naphthodithiophene (NDT) [16,17], and dithienothiadiazole[3,4-c]pyridine [18], have been reported as promising candidates for donor and acceptor units in some of the high performing materials. Oligothiophene derivatives based on bithiophene with unsaturated bonds [19], fluorene based materials [20], platinum containing poly(aryleneethylenes) [21] have been proven to be excellent materials in bulk hetero junction. All these materials provide a clear tendency to form a large orbital overlapping area, which is useful for charge carrier transport.

In the present work, we report the design, synthesis, characterization and transistor application of the novel conjugated polymer **PBDTDPP**, containing benzo[1,2-b:4,5-b′]dithiophene (BDT) donor and diketopyrrolopyrrole (DPP) acceptor chromophore, obtained *via* Stille reaction, as shown in Scheme 1. Due to the presence of triisopropylsilylethynyl in the donor and ethyl hexyl alkyl chain on the DPP acceptor, the polymer **PBDTDPP** exhibited good solubility in common processing solvents for fabrication of OFET such as chloroform, chlorobenzene and O-dichlorobenzene for fabrication of OFETs. While employing **PBDTDPP** as an active layer in a bottom gate/top contact based OFET, the device demonstrated the hole mobility of $9.34 \times 10^{-2}\ cm^2\ V^{-1}\ s^{-1}$ with the On/Off ratio of ~10^4.

2. Experimental

2.1. Materials

Dimethylformamide (DMF), tetrakis(triphenylphosphine)palladium, toluene (99.8%, anhydrous), chloroform, hexane, methanol were purchased from Aldrich. All chemicals were used without further purification. The monomers 2,6-Bis(trimethyltin)-4,8-bis(dimethylsilyloctyl)-benzo[1,2-b:4,5-b′]dithiophene [22] and 2,5-bis(2-ethylhexyl)-3,6-bis(5-bromothiophen-2-yl)pyrrolo[3,4-c]-pyrrole-1,4-dione [23] were prepared by previously described methods.

2.2. Material characterization

UV–Vis absorption spectra were recorded using Lambda 20 (Perkin Elmer) diode array spectrophotometer. All solution in UV–Vis experiments were run in $CHCl_3$. Films were prepared by spin-coating the polymer in $CHCl_3$ solutions onto quartz substrates. ^1H NMR spectra is obtained with a Bruker DPX-300 NMR spectrometer using commercial NMR solvents obtained from Aldrich with TMS as internal standard and chemical shifts are mentioned in δ ppm scale. Cyclic voltametry were performed using Weis-500 work station in a standard three-electrode cell in one-compartment configuration equipped with Ag/Ag^+ electrode, Pt wire, and Pt electrode (diameter 1.6 mm) as the pseudo reference, counter electrode, and working electrode, respectively. The measurements were carried out in anhydrous acetonitrile with tetrabutylammonium hexafluorophosphate (0.1 M) (Bu_4NPF_6) as the supporting electrolyte under an argon atmosphere at a scan rate of 50 mV s^{-1}. Polymer film was prepared by drop-casting onto the Pt working electrode from chloroform solution and dried before measurements. The electrochemical onsets were determined at the position where the current starts to differ from the baseline, and thereby the highest occupied molecular orbital (HOMO) and the lowest unoccupied molecular orbital (LUMO) of polymer were determined. Thermogravimetric analysis (TGA) was performed under a nitrogen atmosphere at a heating rate of 10 °C min^{-1} with a Dupont 9900 analyzer. Samples were run under N_2 and heated from room temperature to 600 °C at a rate of 10 °C/min. Biotage microwave reactor was used for polymerization reaction. The Electrical characteristics of the polymer OFET was measured using a Keithley 4200 parameter analyzer on a probe station in a nitrogen filled glove box. The surface microstructures were examined using non-contact mode atomic force microscopy (Nanoscope, Veeco Instruments, Inc.). A Rigaku RINT 2000 X-ray diffractometer (XRD) with Cu K_α radiation was used to investigate the structural ordering and crystallinity of the polymer films. For this, the polymer films were spin-coated on the SiO_2/Si substrates (300 nm).

2.3. Fabrication and characterization of the organic thin film transistors (OTFTs)

Heavily doped Si substrate was used as gate electrode with 300 nm thick SiO_2 as gate insulating layer. Prior to deposition of polymer, substrates were thoroughly cleaned with deionized water, ethanol and acetone followed by 2 min UV ozone treatment to make the surface hydrophilic. The semiconducting polymer layer from the chlorobenzene solution was spin-coated onto the SiO_2/Si substrate with a concentration of 5 mg/mL. Samples were then dried at 80 °C for 10 min on hot plate in ambient conditions. 50 nm thick of Au electrodes were deposited as source and drain through a metal shadow mask (channel length = 50 μm and width = 1000 μm) *via* thermal evaporator. All the electrical characterizations were performed in dark under ambient air using semiconductor parameter analyzer Agilent 4155 C.

2.4. Synthesis of poly[(5,5'-(benzo[1,2-b:4,5-b']dithiophene-4,8-diyl)bis(thiophene-5,2-diyl))bis (dimethyl(octyl)silane)-2,5-bis(2-ethylhexyl)-3,6-dithiophen-2-yl-pyrrolo[3,4-c]pyr role-1,4-dione] (*PBDTDPP*)

5,5'-(2,6-bis(trimethylstannyl)benzo[1,2-b:4,5-b']dithiophene-4,8-diyl)bis(thiophene-5,2-diyl) bis(dimethyl(octyl)silane (**1**) (302 mg, 0.3 mmol), 2,5-bis(2-ethylhexyl)-3,6-bis(5-bromothiophen-

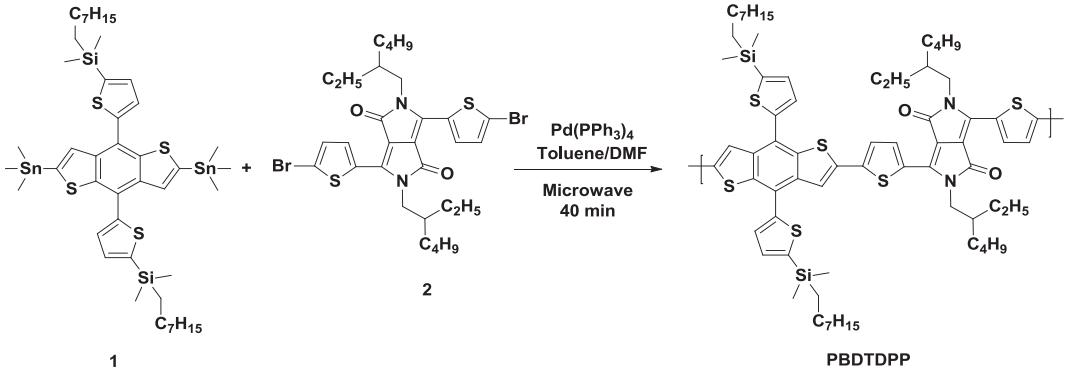

Scheme 1. Synthetic route for polymerization.

2-yl)pyrrolo[3,4-c]-pyrrole-1,4-dione (**2**) (204 mg, 0.3 mmol) and $Pd(PPh_3)_4$ (14 mg, 0.05 eq.) were added to a 20 mL microwave vial. To this, anhydrous DMF (1 mL) and anhydrous toluene (4 mL) were added. The polymerization was carried out at 120 °C for 5 min, 140 °C for 5 min and 170 °C for 30 min. The reaction mixture was cooled to about 50 °C and added slowly to a vigorously stirred methanol (50 mL). The polymer fibers were collected by filtration. The polymer was dissolved in chlorobenzene and precipitated again in methanol. The precipitate was then subjected to Soxhlet extraction with methanol, acetone, hexanes, and chloroform. The final polymer was obtained by evaporation of chloroform and precipitating in methanol. The polymer is filtered and dried in vacuum at 40 °C for 12 h. Finally, dark blue material (330 mg, 92%) was obtained, with the following NMR analysis details: ^1H NMR ($CDCl_3$, 300 MHz, δ/ppm): 8.65 (br, 2H), 7.5 (br, 2H), 7.41–7.40 (br, 2H), 7.23 (br, 2H), 7.20–7.19 (br, 2H), 3.95 (br, 4H), 1.83 (br, 2H), 1.42 (br, 42H), 1.39–1.25 (br, 16H), 1.09–1.06 (br, 20H), 0.86 (br, 12H), 0.46 (br, 18). 0.31–0.12 (br, 12H). Anal.calcd: C, 67.16; H, 7.46; N, 2.30, S, 15.82; found C, 67.14; H, 7.38; N, 2.28, S, 15.80.

3. Result and discussion

3.1. Synthesis and characterization

PBDTDPP conjugated polymer was synthesized in microwave following the $Pd(PPh_3)_4$ catalyzed Stille copolymerization using 2,6-bis(trimethyltin)-4,8-bis(5-(dimethyl-octylsilyl)thiophene-2-yl)benzo[1,2-b:4,5-b']dithiophene and 2,5-bis(2-ethylhexyl)-3,6-bis(5-bromothiophen-2-yl)pyrrolo[3,4-c]-pyrrole-1,4-dione, as monomers. Synthetic route for the copolymerization is illustrated in Scheme 1. To facilitate the solubility of the corresponding polymer, silyl alkyl side chain group was introduced to benzodithiophene and ethyl hexyl group on DPP monomer. The crude polymer was extracted with chloroform, collected by precipitation in methanol, and extracted with methanol and acetone, successively using Soxhlet apparatus to remove the byproducts. The number average molecular weights (M_n) and polydispersity indices (PDI) of the copolymer was determined by the gel permeation chromatography (GPC) analysis with a polystyrene standard calibration in chloroform eluent and is found to be 50.7 kg mol^{-1} with a poly dispersity index of 2.7 (Table 1). The structures of the polymer is characterized and confirmed by their elemental analysis. The polymer is highly soluble in chloroform, chlorobenzene and o-dichlorobenzene, which is important criteria for device processing.

Thermal stability of polymer is a very important criterion for their use in electronic devices. Fig. 1 shows the TGA, revealing the onset temperature with 5% weight loss (T_d) of **PBDTDPP** above 303 °C. This indicates that the polymer have good thermal stability, and is suitable for robust organic electronic devices. Photophysical properties are summarized in Table 1.

3.2. Optical properties

In order to determine the optical properties of the polymer **PBDTDPP,** the thin films were deposited on quartz plates. Prior to deposition, the quartz plates were cleaned thoroughly with deionized water, chloroform and acetone followed by drying in an oven. The semiconducting polymer layer was spin-coated from the chloroform solution with a concentration of 5 mg mL^{-1}. The films were dried at 80 °C. The absorption spectra exhibited by the polymer in chloroform solution and the thin film is shown in Fig. 2. The entire absorption spectra features broad absorption bands with the wavelength ranging from 300 nm to 900 nm. The absorbance bands in chloroform solution were observed at 690 nm and 750 nm, whiles for thin films the absorption bands appeared at 700–765 nm. The polymer films were slightly red-shifted by 10–15 nm, which could most likely to be due to high coplanarity or enhanced intermolecular electronic interactions in the solid state that leading the stability to a lower energy excited state. The higher energy absorbances were attributed to the localized π-π* transitions, while the lower energy bands were associated with an intramolecular charge transfer (ICT) between the donor and acceptor similar to those characterized by Jespersen et al. [24,25]. Optoelectronic properties including the maximum absorption peak wavelengths (λ_{max}) and the optical band gap (E_g^{opt}) are summarized in Table 2. Based on the absorption edges (λ_{onset}), the optical band gap (E_g^{opt}) of the **PBDTDPP** is estimated to be about 1.31 eV.

Table 1
Physical properties of the polymer.

Polymer	M_n[a] [kg/mol]	Mw[a] [kg/mol]	PDI	Yield [%]	T_d[b] [°C]
PBDTDPP	50.5	147.8	2.7	91	303

[a] Molecular weights were determined by using gel permeation chromatography (GPC) against polystyrene standards in chloroform as eluent.
[b] Temperature resulting in 5% weight loss based on initial weight.

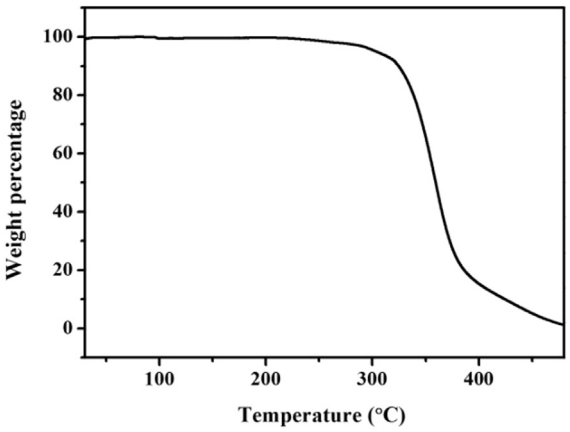

Fig. 1. TGA plots for the polymer, obtained with a heating rate of 10 °C min^{-1} under an inert atmosphere.

3.3. Electrochemical properties

Cyclic voltammetry of the **PBDTDPP** was studied for determining the highest occupied molecular orbital (HOMO) and the

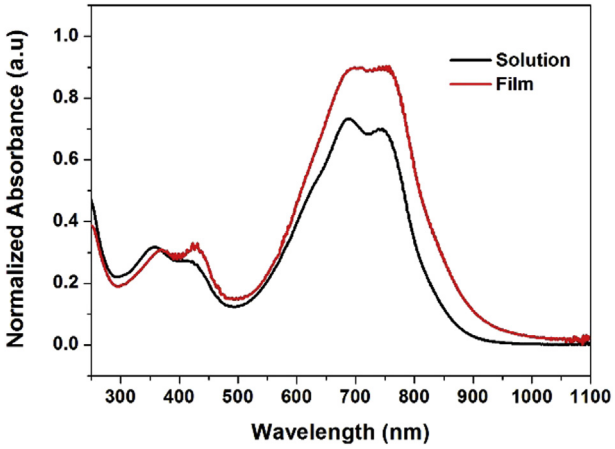

Fig. 2. UV–Vis absorption spectra of the PBDTDPP in chloroform solution and in thin film.

Table 2
Optical and electrochemical properties of the polymer.

Polymer	λ_{max}[a] (Sol) (nm)	λ_{max}[a] (Film) (nm)	HOMO[b] (eV)	LUMO[c] (eV)	E_g^{opt}[d] (eV)
PBDTDPP	690, 750	700, 765	−5.42	−4.11	1.31

[a] UV–Vis absorption spectra of the polymer were measured in chloroform solution and thin film.
[b] HOMO levels of the polymer were determined from onset voltage of the first oxidation potential with reference to ferrocene at −4.8 eV.
[c] LUMO levels of the polymer were estimated from the optical band gaps and the HOMO energy levels.
[d] Optical band gap was calculated from the UV–Vis absorption onset in film.

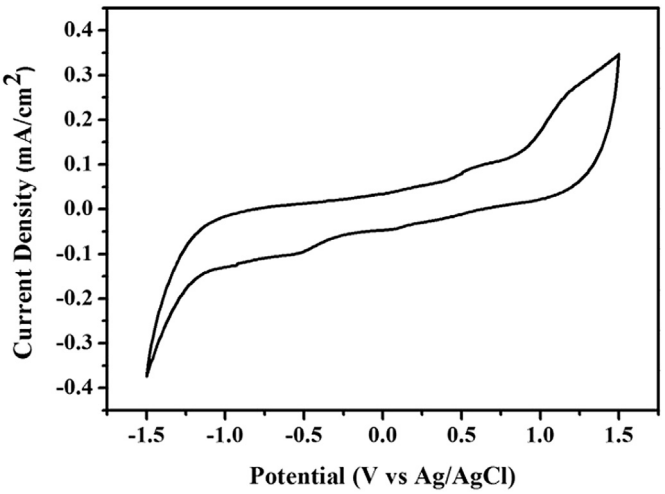

Fig. 3. Cyclic voltammograms of PBDTDPP in 0.1 M Bu_4NPF_6/CH_3CN, scan rate 50 mV s^{-1}, Pt working electrode.

lowest unoccupied molecular orbital (LUMO) energy levels. Herein, the onset oxidation and reduction potentials of the voltammogram correspond to HOMO and LUMO energy levels, respectively. As shown in Fig. 3, the onset oxidation potential (E_{ox}) of the **PBDTDPP** is at 0.87 versus Ag/Ag^+ reference electrode. Using the ferrocene reference value of −4.8 eV below the vacuum level [25], the HOMO energy level of the polymer is calculated as $E_{HOMO} = -(E_{ox} - E_{Fc} + 4.8)$ (eV), wherein E_{Fc} is the potential of the internal standard for the ferrocene/ferrocenium ion (Fc/Fc^+) couple. The value of E_{Fc}, which was determined under the same experimental conditions, was approximately 0.25 eV vs Ag/Ag^+. Thus, the HOMO level was determined to be −5.42 eV. Further, using the optical band gap E_g^{opt} and the HOMO energy level and following the equation $E_{LUMO} = E_{HOMO} + E_g^{opt}$ [25], the LUMO energy level of the **PBDTDPP** was estimated to be −4.11 eV. The results are summarized in Table 2. The **PBDTDPP** shows a deeper HOMO energy level of −5.42eV, which indicates the presence of strong π-π stacking among the polymer backbone and the formation of ordered arrangements in their solid films. The polymer demonstrates promising optical and electrochemical properties and gives a clear red shift.

3.4. Organic filed effect transistors (OFET)

The electrical properties of the material was examined by fabricating OFETs, Fig. 4 illustrates typical transfer and output characteristics of the OFET using **PBDTDPP** as an active channel. A Top contact-bottom gate (BG/TC) device geometry (Fig. S1) with Si(gate), SiO_2(gate dielectric layer) and Au (contact electrode), was adopted to probe the charge transport properties of the polymer in OFETs devices. The field effect mobility was obtained from the source–drain current–gate voltage curves (I_{DS} versus V_G) at a drain voltage of −50 V in well-resolved saturation regions. The hole mobility of polymer in the saturation region [18] was calculated using following equation,

$$I_{ds}=(WCi/2L)\mu(V_G\text{-}V_T)^2 \quad (1)$$

where I_{ds} is the drain-source current in the saturated region, W and L are the channel width and length, respectively, μ is the field-effect mobility, C_i is the capacitance per unit area of the insulation layer (SiO_2, 300 nm), and V_G and V_T are the gate and threshold voltages, respectively. All devices exhibited a typical p-channel transistor behaviour and a well saturating output characteristics as shown in Fig. 4. Maximum field effect mobility of the **PBDTDPP** in saturation region was found to be ~9.34×10^{-2} $cm^2V^{-1}S^{-1}$ with the ON/OFF ratio of more than ~10^4 and the threshold voltage of −11.8 V (Drain voltage $V_D = -50$ V).

Table 3, shows the summarized **PBDTDPP** based FET characteristics. These results clearly demonstrate that both the backbone and side chains of the polymer have a great influence on the corresponding OFET performance. Thus, the exhibited electrical properties can be attributed to the coplanarity of **PBDTDPP** polymer that results into layer by layer self-assembly during spin

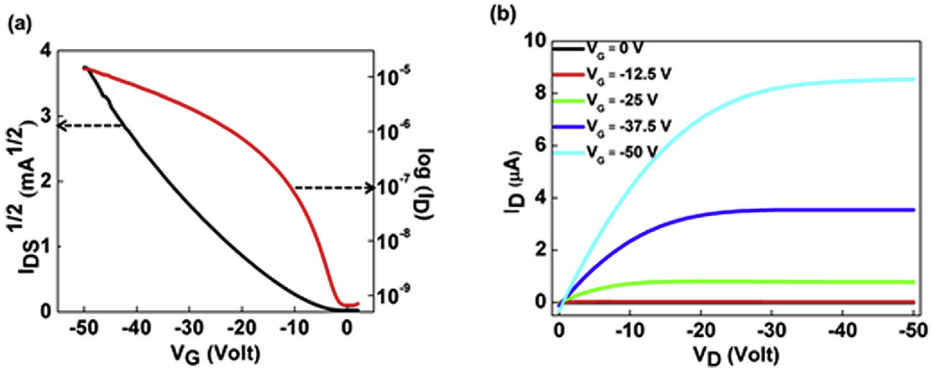

Fig. 4. Transfer characteristics of OFET fabricated with Polymer PBDTDPP at $V_D = -50$ V.

Table 3
Device characteristics of solution processed OFET.

Polymer	μ_{max} [$cm^2V^{-1}s^{-1}$]	[a]I_{on}/I_{off}	Threshold Voltage(V_D)	Drain Voltage(V)
PBDTDPP	9.34×10^{-2}	10^4	–11.8 V	–50 V

[a] I_{on}/I_{off} refers to the corresponding on-to-off ratio and the threshold voltage at the maximum hole mobility.

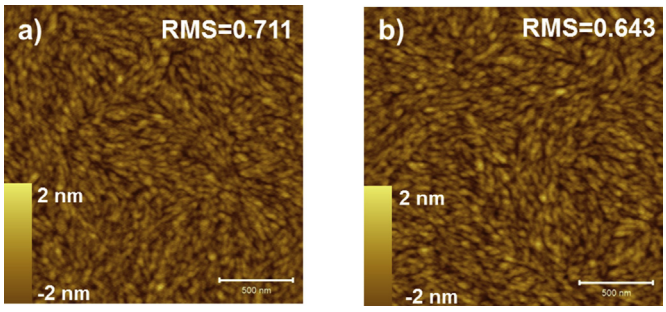

Fig. 5. Atomic force microscopy (AFM) topography (a) and (b) at pristine and 150 °C.

coating process. This ultimately results in improving on current which evidently improves mobility and the On/Off ratio. These results clearly demonstrates **PBDTDPP** polymer as a potentially viable candidate for OFETs application. The crystallinity of the material was probed by X-ray diffraction analysis at different annealing temperatures as shown in Fig. S2. However, the polymer material was observed to be amorphous in nature presumably due to its longer silyl alkyl chain, which might have rendered the material in such a state [18]. Fig. 5 and Fig. S3 show the surface topography and phase images, respectively of the polymer in its pristine state and after annealing at 150 °C. The material shows a terrance-like morphology in its pristine state with a surface roughness (RMS) of ~0.711 nm. Annealing aided in a much improved surface roughness of ~0.643 nm, which is quite beneficial for charge transport.

4. Conclusion

In summary, novel low band gap conjugated polymer based on the silylthiophene substituted benzodithiophene and diketopyrrolopyrrole was synthesized and employed as an active layer for OFETs application. The polymer exhibited a rather deep HOMO and LUMO energy levels and readily soluble in commonly employed organic solvents. Applying the polymer as an active channel in OFETs resulted in a mobility as high as 9.34×10^{-2} cm^2 V^{-1} S^{-1}. This result demonstrates the potential application of the silylthiophene substituted benzodithiophene and diketopyrrolopyrrole copolymer in OFETs application. Additional modifications to the polymer structure and device are currently under study for further enhancing the device performance.

Acknowledgements

This work was supported by Dongguk University-Seoul Research Fund (2017) and by the Nano·Material Technology Development Program through the National Research Foundation of Korea (NRF) funded by the Ministry of Science, ICT & Future Planning (MSIP, Korea) (2014M3A7B4051745).

Appendix A. Supplementary data

Supplementary data to this article can be found online at https://doi.org/10.1016/j.jorganchem.2018.11.013.

References

[1] G. Gelinck, P. Heremans, K. Nomoto, T.D. Anthopoulos, Adv. Mater. 22 (2010) 3778–3798.
[2] T. Someya, A. Dodabalapur, J. Huang, K.C. See, H.E. Katz, Adv. Mater. 22 (2010) 3799–3811.
[3] A. Facchetti, Mater. Today 10 (2007) 28–77.
[4] G. Yu, J. Gao, J.C. Hummelen, F. Wudl, A.J. Heeger, Science 270 (1995) 1789–1791.
[5] S.H. Park, A. Roy, S. Beaupré, S. Cho, N. Coates, Ji S. Moon, D. Moses, M. Leclerc, K. Lee, A.J. Heeger, Nat. Photon. 3 (2009) 297–302.
[6] A.J. Heeger, Adv. Mater. 26 (2014) 10–28.
[7] R.C. Coffin, J. Peet, J. Rogers, G.C. Bazan, Nat. Chem. 1 (2009) 657–661.
[8] Kang, H.-J. Yun, D.S. Chung, S. Z-Ki Kwon, Y-Hi Kim, J. Am. Chem. Soc. 135 (2013) 14896–14899.
[9] C. Bathula, S. Badgujar, N.S. Belavagi, S.K. Lee, Y. Kang, I.A.M. Khazi, J. Fluoresc. 26 (2016) 371–376.
[10] Ji-H. Kim, M. Lee, H. Yang, Do-H. Hwang, J. Mater. Chem. 2 (2014) 6348–6352.
[11] Y. Li, S.P. Singh, P. Sonar, Adv. Mater. 22 (2010) 4862–4866.
[12] Y. Liang, Z. Xu, J. Xia, S.-T. Tsai, Y. Wu, G. Li, C. Ray, L. Yu, Adv. Mater. 22 (2010) E135–E138.
[13] H. Zhou, L. Yang, A.C. Stuart, S.C. Price, S. Liu, W. You, Angew. Chem. Int. Ed. 50 (2011) 2995–2998.
[14] S.C. Price, A.C. Stuart, L. Yang, H. Zhou, W. You, J. Am. Chem. Soc. 133 (2011) 4625–4631.
[15] C. Bathula, M. Kim, C.E. Song, W.S. Shin, D.-H. Hwang, J.-C. Lee, I.-N. Kang, S.K. Lee, T. Park, Macromolecules 48 (2015) 3509–3515.
[16] S. Badgujar, C.E. Song, W.S. Shin, S.-J. Moon, I.-N. Kang, J. Lee, S. Cho, S.K. Lee, Jong-Cheol Lee, Macromolecules 45 (2012) 6938–6945.
[17] C. Bathula, C.E. Song, S. Badgujar, S.-J. Hong, S.Y. Park, W.S. Shin, J.-C. Lee, S. Cho, T. Ahn, S.-J. Moon, S.K. Lee, Polym. Chem. 4 (2013) 2132–2139.
[18] C. Bathula, S.K. Lee, P. Kalode, S. Badgujar, N.S. Belavagi, I.A.M. Khazi, Y. Kang, J. Fluoresc. 26 (2016) 1045–1052.
[19] C. Cui, Y. Wu, C.-L. Ho, Q. Dong, Z. Lin, Y. Li, W.-Y. Wong, Chem. Asian J. 11 (24) (2016) 3557–3567.
[20] L. Liu, C.-L. Ho, W.-Y. Wong, K.-Y. Cheung, M.-K. Fung, W.-T. Lam, A.B. Djurišić, W.-K. Chan, Adv. Funct. Mater. 18 (2008) 2824–2833.
[21] W.-Y. Wong, X.-Z. Wang, Z. He, K.-K. Chan, A.B. Djurišić, K.-Y. Cheung, C.-T. Yip, A.M. Ching Ng, Y.Y. Xi, C.S.K. Mak, W.-K. Chan, Am. Chem. Soc 46 (2007) 14372–14380.
[22] N. Chakravarthi, K. Gunasekar, C.S. Kim, D.-H. Kim, M. Song, Y.G. Park, J.Y. Lee, Y. Shin, I.-N. Kang, S.-H. Jin, Macromolecules 48 (2015) 2454–2465.
[23] L. Dou, J. Gao, E. Richard, J. You, C.-C. Chen, K.C. Cha, Y. He, G. Li, Y. Yang, J. Am. Chem. Soc. 134 (2012) 10071–10079.
[24] K.G. Jespersen, W.J.D. Beenken, Y. Zaushitsyn, A. Yartsev, M. Andersson, T. Pullerits, V. Sundström, J. Chem. Phys. 121 (2004) 12613–12617.
[25] C.-H. Yang, Y.-K. Sun, Y.-Y. Chuang, T.-L. Wang, Y.-T. Shieh, W.-J. Chen, Electrochim. Acta 69 (2012) 256–267.